

Design and thermal analysis of partial ceramic coated piston of spark ignition (SI) Engine

R.Silambarasan¹, S.Balakrishnan², A.Selvarasu³

Assistant Professor, VSB Engineering College, Karur, Tamilnadu^{1,2,3}

Abstract: This paper is to determine the temperature and the stress distributions in a partial ceramic coated spark ignition (SI) engine piston and reduce the mass of the piston for improving engine operating parameters. Our aim of this paper is to determine the temperature and the stress distributions in a partial ceramic coated spark ignition (SI) engine piston. Influence of structure, coating thickness and distributions of stress and temperature were investigated including comparisons with results from an uncoated piston. Thermal analysis is investigated on a conventional (uncoated) SI engine piston, made of steel and Al-Si alloy. Then, thermal analysis is performed on MgO-ZrO₂ coated piston by using ANSYS 11.0. Finally, the results of existing piston and modified piston have been compared in order to improve the piston life and weight.

Keywords: Design; Piston; Mgo-Zro₂; Thermal; ANSYS

I. INTRODUCTION

The thermal barrier coating and constructional change to the aluminum piston crown results in a reduction in the temperature of substation which may be possible to return the aluminum piston to historic durability levels at the higher engine output. The analysis should be needed a clear definition of the material properties, selection of element, boundary conditions and initial conditions [2]. For which the certain data are calculated using the petrol engine cycle and some are taken from the literatures. All the data assumed in the analysis are theoretical values and hence the analysis is purely theoretical. With the analysis done the results are used to fix a benchmark for carrying out the experimental analysis with the coating of a thermal barrier (PSZ in this case) as shown in table 1.

TABLE 1 properties of cast aluminum alloy

Material property	Al Alloy
Thermal conductivity, k (W/mK)	155
Density, ρ (kg/m ³)	2700
Specific heat, C (J/kg K)	965
Coefficient of thermal expansion (1/°C)	19.5×10 ³
Young's modulus, E (Mpa)	90×10 ³
Yield strength (Mpa)	410
Poisson's ratio	0.3

The piston is made of cast aluminum alloy (Al - Si). Its material property is presented in table 1 it has good strength and hardness at elevated temperatures with good wear resistance.

II. 2. COMPONENT MODELING

The piston is modeled in PRO-E WILDFIRE-4.0, which is one of the most effective modeling packages. IGES (Initial Graphics Exchange Specification) is the ANSI standard

A Finite element meshing and analysis

Using SOLID 70 brick element [7] it is meshed as shown in fig.3. As temperature gradients are higher in the

that defines a natural format for the exchange of information between CAD/CAM systems with an IGES translator. The both existing and modified piston was modeled in PRO-E wildfire 4.0 which are shown in fig. 1 and fig.2.

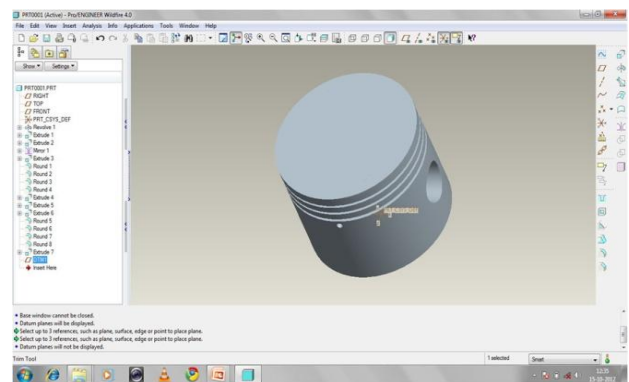


Fig. 1 Existing Piston

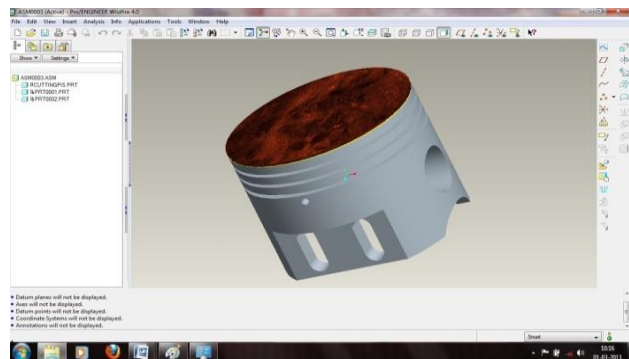


Fig. 2 Modified Piston

combustion chamber therefore a relatively fine mesh is used at the combustion chamber so, the element size gradually increases.

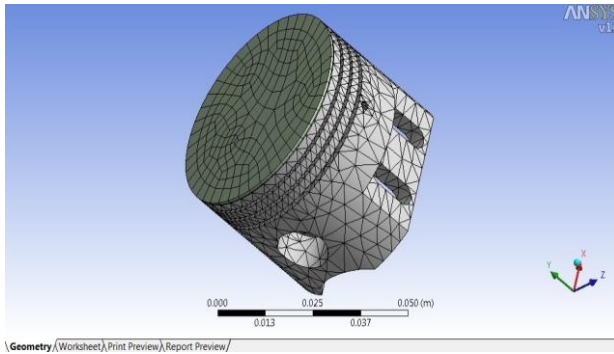


Fig 3 Meshed View

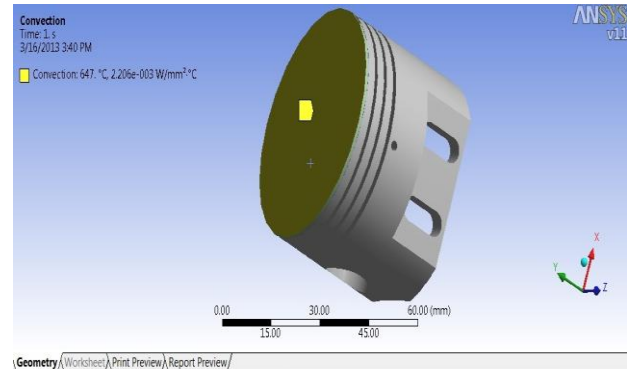


Fig 4 Boundary Condition at Piston Crown

B Post processing

The boundary conditions are applied to solve the problem using the Ansys 11.0 solver. The following results were obtained like temperature distribution, heat flux, deflection and total stress.

C Solution phase

In this phase, initial conditions, boundary conditions and thermal loads are applied as explained below and finally solved to obtain results.

Initial and boundary conditions includes thermal and structural conditions. Since the problem is a steady state analysis, the initial condition is the temperature of the piston body only. The initial temperature of the piston is assumed to be 60°C (333K). This assumption is taken with the base that the lubricating oil has the least temperature and acts as the main sink in the system and hence the initial piston temperature at steady state is assume to be equal to the lubrication oil temperature.

III. THERMAL ANALYSIS AND THERMAL BOUNDARY CONDITION

There are four boundary conditions applied to the model i.e. four convectational heat transfers occurring during the analysis. They are shown in the fig. 4 to fig. 8 below. The first region is the piston head indicated in red. This is where the combustion occurs. Here convectational heat transfer occurs from the working medium to the piston.

The working medium above the piston contains a mixture of compressed air, un-burnt fuel and burnt gases at eh moment when the combustion begins. But during that time it is assumed that there would be layers created as shown below. Hence an assumption is made that there would be a one millimeter thin layer of compressed air present over the piston surface. With this a model of a thin air cap having same contour of the piston head is made to find the effective temperature of the gas touching the piston for convection. The model is analyzed in Ansys with the boundary conditions as shown in the fig. 4

The temperature required to determine the boundary conditions is calculated based on the theoretical Otto cycle and the heat transfer coefficient acting on the top of the piston is calculated by the governing equation.

$$h_{gas} = C_1 V_c^{-0.06} P^{0.8} T^{-0.4} (V_p + C_2)^{0.8}$$

At the end of compression

$$h_{gas} = 1736.9985 \frac{W}{m^2 K}$$

Where,

C1 – Constant = 130

C2 – Constant = 1.4

Vc – Instantaneous cylinder volume (m3)

Vp – Mean Piston Speed (m/sec)

T – Instantaneous Mean Gas Temperature (K)

P – Instantaneous Cylinder Pressure (Mpa)

A Temperature distribution

The below fig. 5 shown gives the temperature distribution over the volume of the piston at steady state after and application of thermal loads. The maximum temperature occurs at the top of the piston. A ‘MAX’ symbol on the temperature distribution chart shows the maximum temperature point. The minimum temperature occurs at the bottom, it is indicated by ‘MIN’. An interesting feature in this temperature distribution chart is the combustion chamber. Even though the working medium is at the higher temperatures, the surface temperature at the combustion temperature is comparatively low.

B Heat flux

The fig 5 & fig 6 shown above gives the thermal flux distribution over the volume of the piston at steady state after the application of thermal loads. The maximum heat flux occurs at the first ring of the piston. A ‘MAX’ symbol on the heat flux distribution chart shows the maximum heat flux point. The minimum heat flux occurs at the bottom, it is indicated by ‘MIN’. An interesting feature in this heat flux distribution chart is the piston ring. Even though the heat transfer co- efficient on the piston ring is very low, the heat flux seems to be very high and increases sharply near the edge of the first ring (compression ring). Similarly there is a maximum heat flux in the interior region, i.e. in the edges below the combustion chamber.

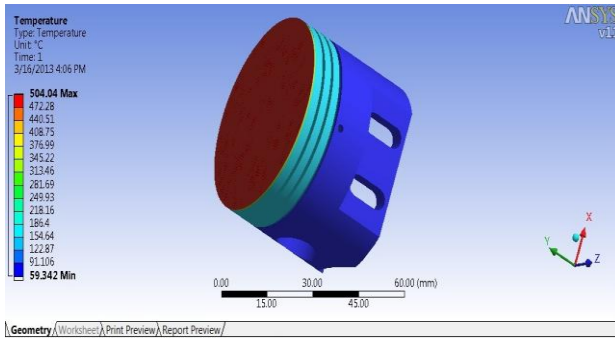


Fig. 5 Temperature Distribution

C Total heat flux

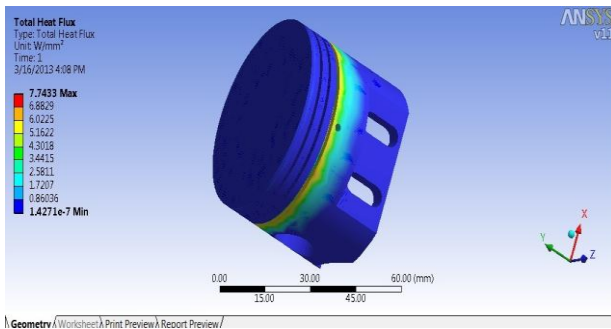


Fig. 6 Total Heat Flux

D Directional heat flux

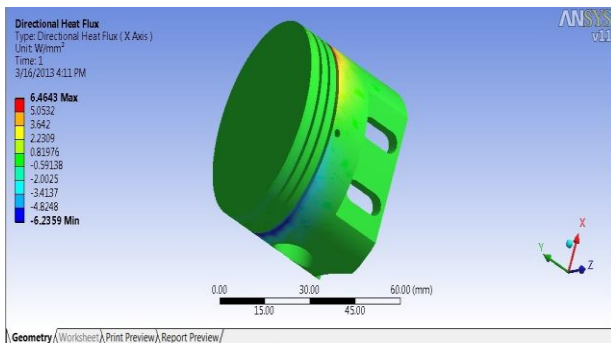


Fig 7 Directional Heat Flux

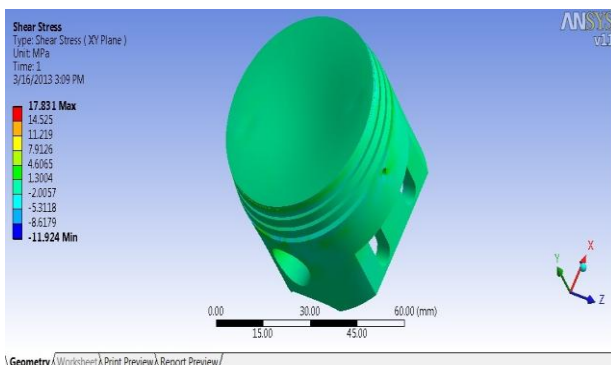


Fig. 8 Shear Stress

IV. SHEAR STRESS

A shear stress, denoted τ is defined as the component of stress coplanar with a material cross section. Shear stress arises from the force vector component parallel to

the cross section. Normal stress, on the other hand, arises from the force vector component perpendicular or anti parallel to the material cross section on which it acts. The fig 7 & fig 8 shown above gives the directional heat flux distribution and shear stress over the volume of the piston at steady state after the application of thermal loads which are given in table 3.

C Stress intensity

The stress intensity factor, K , is used in fracture mechanics to predict the stress state ("stress intensity") near the tip of a crack caused by a remote load or residual stresses. The value of stress intensity value is given in table 4 and whose image is shown in fig 9. It is a theoretical construct usually applied to a homogeneous, linear elastic material and is useful for providing a failure criterion for brittle materials, and is a critical technique in the discipline of damage tolerance. The concept can also be applied to materials that exhibit small-scale yielding at a crack tip. The magnitude of K depends on

$$\sigma_{ij}(r, \theta) = \frac{K}{\sqrt{2\pi r}} f_{ij}(\theta) + \text{higher order terms}$$

Where K the stress intensity is factor (with units of stress \times length^{1/2}) and f_{ij} is a dimensionless quantity that depends on the load and geometry. This relation breaks down very close to the tip (small r) because as r goes to 0, the stress σ_{ij} goes to ∞ . Plastic distortion typically occurs at high stresses and the linear elastic solution is no longer applicable close to the crack tip. However, if the crack-tip plastic zone is small, it can be assumed that the stress distribution near the crack is still given by the above relation. sample geometry, the size and location of the crack, and the magnitude and the modal distribution of loads on the material. Linear elastic theory predicts that the stress distribution (σ_{ij}) near the crack tip, in polar coordinates (r, θ) with origin at the crack tip, has the form.

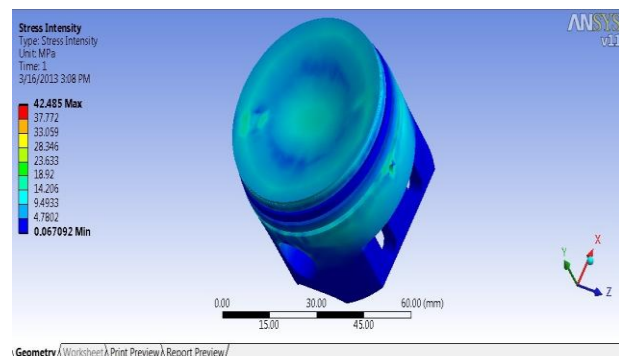


Fig. 9 Stress Intensity

A Principle stress

The maximum and minimum stress occurring on the principal planes where no shear stress occurs are known as principal stresses. The stress and strain as shown in fig 10

to fig 15 and the Maximum and Minimum value is given in table 4.

B Maximum principle stress and Normal stress

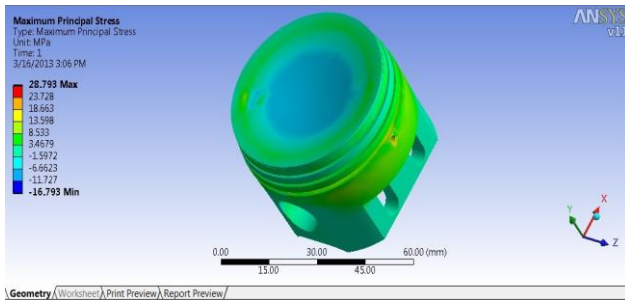


Fig .10 Maximum Principle Stress

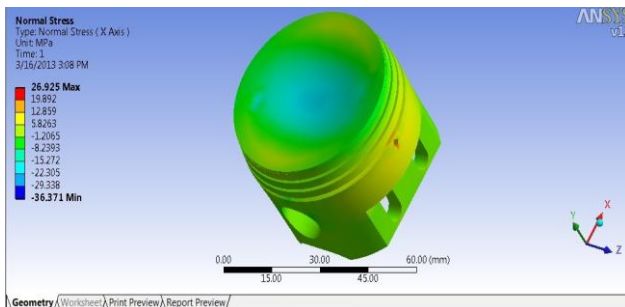


Fig. 11 Normal Stress

D Equivalent stress

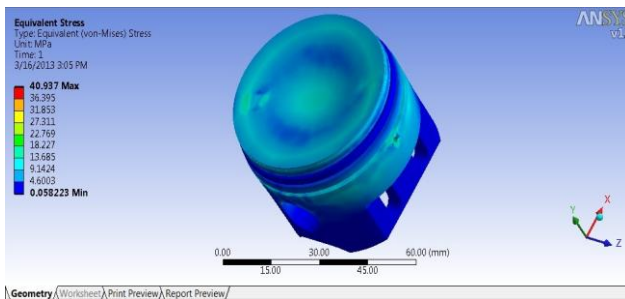


Fig. 12 Equivalent Stress

E Maximum shear stress

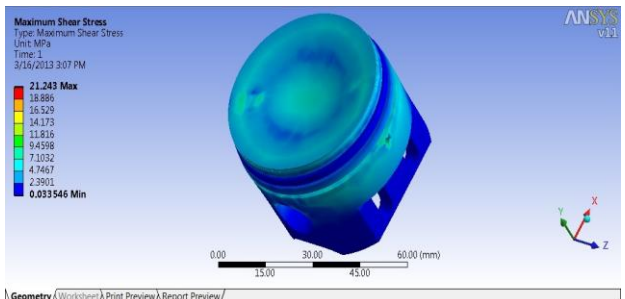


Fig. 13 Maximum Shear Stress

E Maximum principle elastic strain

A Thermal analysis

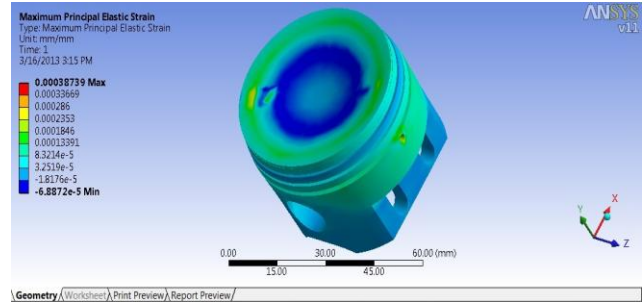


Fig. 14 Maximum Principle Elastic Strain

F Minimum principle elastic strain

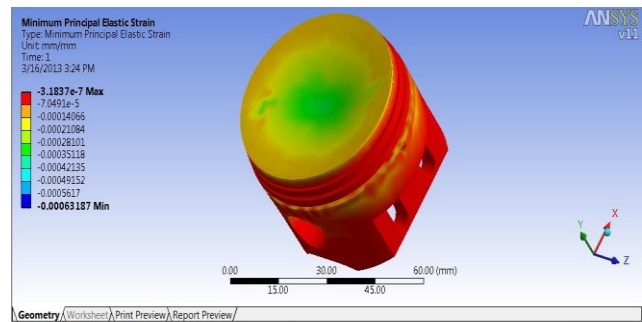


Fig. 15 Minimum Principle Elastic Strain

V. STRAIN ENERGY

In fig 16 shows a molecule, strain energy is released when the constituent atoms are allowed to rearrange themselves in a chemical reaction or a change of chemical conformation in a way that:

- Angle strain,
- Torsional strain,
- Ring strain and/or Steric strain,
- Allylic strain, and
- Pentane interference

The external work done on an elastic member in causing it to distort from its unstressed state is transformed into strain energy which is a form of potential energy.

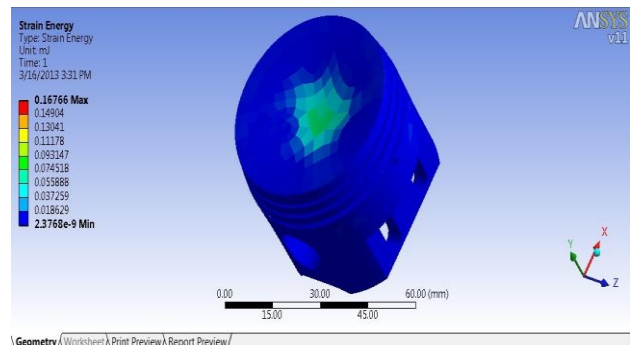


Fig 16 Strain Energy

TABLE 3 THERMAL ANALYSIS

Properties	Directional Heat Flux (W/mm ²)		Total Heat Flux (oC)		Temperature Distribution (W/mm ²)	
	MAX	MIN	MAX	MIN	MAX	MIN
Existing Piston	0.0052658	-0.006965	0.0114	0.00057086	450	159.05
Modified Piston	6.4643	-6.2359	7.7433	1.4271×10 ⁻⁷	504.04	59.342

B Structural analysis

TABLE 4 STRUCTURAL ANALYSIS

Properties	Directional Deformation (mm)		Equivalent Stress (MPa)		Maximum Principle Elastic Strain (mm/mm)	
	MAX	MIN	MAX	MIN	MAX	MIN
Existing Piston	1.1457	-1.1125×e-9	4.2078×e-5	6.5143×e-8	1.3659×e-10	-6.6743×e-12
Modified Piston	0.0035151	-0.0035635	40.937	0.058223	0.00038739	-6.8872×e-5

Properties	Maximum Principle Stress (MPa)		Maximum Shear Stress (MPa)		Minimum Principle Elastic Strain (mm/mm)	
	MAX	MIN	MAX	MIN	MAX	MIN
Existing Piston	2.7481×e-5	-9.8709×e-6	2.1395×e-5	3.5270×e-8	-1.2e-13	-2.14
Modified Piston	28.793	-16.793	0.033543	21.243	-3.1837e-7	-0.00063187

Properties	Shear Stress (MPa)		Normal Stress (MPa)		Strain Energy (mJ)	
	MAX	MIN	MAX	MIN	MAX	MIN
Existing Piston	9.516×e-6	-1.338×e-5	2.659×e-5	-3.285×e-5	6.847×e-14	6.3715×e-22
Modified Piston	17.831	-11.924	26.925	-36.371	0.16766	2.3768×e-9

Properties	Stress Intensity (MPa)		Total Deformation (m)		Mass (gm)
	MAX	MIN	MAX	MIN	
Existing Piston	4.2789×10 ⁻⁵	7.0548×10 ⁻⁸	5.008	2.377	113.69
Modified Piston	42.485	0.067092	0.014278	2.2011×10 ⁻⁶	109.05

The strain energy in the form of elastic deformation is mostly recoverable in the form of mechanical work.

VI. MASS REDUCTION

Mass reduction = Mass of the Existing piston - Mass of the Modified piston
 = 113.69 – 109.05
 = 4.64 gm

VII. RESULTS AND DISCUSSIONS

We have compared the obtained result of thermal & structural analysis of existing piston and modified piston. The thermal analysis, structural analysis, Stress distributions were calculated and tabulated above.

VIII. CONCLUSION

The existing piston is redesigned using Pro-E software and analyzed by ansys software. The coating of ceramic (magnesium oxide (MgO) and zirconium oxide (ZiO)) over existing aluminum alloy piston is done and behavior is analyzed to improve the performance of the given engine. Thermal analyses results indicate that the coated section of the piston, which is close to the crevice and crown regions, cause an increase in the temperature. It is therefore concluded that this temperature increase leads to an increase in air fuel mixture temperature in these sections and thus unburned charge oxidation near the entrance of the clearance increases. As a result of increase in temperature, a slight amount of decrease in carbon

monoxide emission may be expected since CO oxidation reactions strongly depend on temperature.

REFERENCES

- [1] Bhaumik Patel, Ashwin Bhabhor DESIGN AND PREDICTION OF TEMPERATURE DISTRIBUTION OF PISTON OF RECIPROCATING AIR COMPRESSOR, International journal of Advanced Engineering, IJAERS/Vol. 1/ Issue III/April-June, 2012/172-174
- [2] P. Gustof, A. Hornik The influence of the engine load on value and temperature distribution in the piston of the turbocharged Diesel engine.
- [3] Ekrem Buyukkaya , Muhammet Cerit “Thermal analysis of a ceramic coating diesel engine piston using 3-D finite element method” Surface and coatings technology, June 2007.
- [4] Muhammet Cerit “Thermo mechanical analysis of a partially ceramic coated piston used in an SI engine” ,Surface & coatings Technology, December 2010.
- [5] M.M.Ragman, A.K.Arifin,N.Jamaludin “Fatigue life prediction of two stroke free piston engine mounting using frequency response approach” European journal of scientific research, Vol 22 No.4, 2008.
- [6] Mirowslaw karczewski,Krzysztof kolinski jercy walentynowcisz “Optical analysis of combustion engine elements” journal of KONES Powertrain and transport , Vol 18, No.1, 2011.
- [7] Jing Yang, Yi Wang, “Heat load analysis of piston based on the ANSYS”, Advanced materials research, Vol 199-200, 2011. Ekrem Buyukkaya, Muhammet Cerit, Theoretical analysis of ceramic coated petrol engine piston using finite element method, Sakarya University, Engineering Faculty, Department of Mechanical Engineering, Esentepe Campus, Sakarya 54187, Turkey (2007).
- [8] Imdat Taymaz, The effect of thermal barrier coatings on Petrol engine performance, Faculty of Engineering, University of Sakarya, Esentepe Kampusu, 54178, Adapazan, Turkey (1993).
- [9] Alan Levy and Stuart Macadam, The behavior of ceramic thermal barrier coatings on diesel engine combustion zone components, Lawrence Berkeley Laboratory, University of California, Berkley, CA (1986).